

25th ABCM International Congress of Mechanical Engineering
October 20-25, 2019, Uberlândia, MG, Brazil

COB-2019-0152

EXPERIMENTAL ANALYSIS OF SINGLE AND TWO-PHASE FLOWS THROUGH CHOKE VALVES

Luis Fernando Campuzano Ojeda

Lucas Braga de Mello

Yan Caires Capellaro

Charlie Van Der Geest

Marcelo Souza de Castro

School of Mechanical Engineering, University of Campinas, Rua Mendeleev, 200, Cidade Universitária, Campinas, SP, CEP 13083-860, Brazil

luiscampuzano@gmail.com, lucaomello12@gmail.com, kant.ando@hotmail.com, geest@unicamp.br, mcastro@fem.unicamp.br

Abstract. *On the petroleum industry, in the production, there are single and multiphase flows from the reservoir to the separator through horizontal and vertical lines. Devices such as singularities may increase or decrease fluid kinetics' energy and to control the flow. These singularities are commonly installed for multiple purposes. One type of restrictions are the valves as chokes and orifice plates, some of them are designed to metering, others are for flow control and/or pressure control. The objective of this paper is to show an experimental study of horizontal single and multiphase flow through orifice plates. The single-phase (liquid) and multiphase experiments (liquid/gas) are being performed, using water, oil and air as working fluids. The objective of this paper is to analyze the behavior of the pressure drop and discharge coefficient (C_d) at different orifices diameters using the literature as background, such as applicable norms for single-phase, empirical correlations and homogenous/nonhomogeneous models for multiphase flows. Results obtained on this research will be compared with literature and the fluid behavior for critical flow and subcritical flow.*

Keywords: *Gas-Liquid Flows, Orifice Plates, CHOKE VALVES, Singularities, Multiphase Flow choke models.*

1. INTRODUCTION

In order to safely control an oil and gas production system, it is necessary to understand the multiphase flow behavior through restrictions or singularities such as choke valves. Al-Safran et al. (2017) described the multiphase flow through restrictions, saying that the fluid flow behavior across valves is characterized by a converging fluid flow due to reduction in area, thus, the valves in the production system can be defined as a sudden reduction in cross-sectional area over a short pipe segment. The reduction causes an increase in the fluid velocity for incompressible fluids due to mass conservation. Also, as the fluid velocity increases, the pressure in the reduction decreases due to conservation of energy. The characteristics of valves in the industry are related with their main purpose: dissipate an amount of flow energy to control the flowrate, indeed, a considerable pressure drop occurs across the restriction. The chokes are valves that particularly satisfies these characteristics which is the reason of this experimental work. A choke is a device installed at the wellhead or downhole, used to cause a restriction to the fluid flow, thus controlling the oil and gas production rate. Chokes can be classified as orifice-type, with fixed diameters or adjustable orifice diameters (BRILL, 1970).

To highlight the importance of chokes in the oil and gas production system, we emphasize the choke's basic functions described by Sachdeva et al. (1986). They are used to control and optimized production flowrate from wells and to avoid water or gas coning. Also, the choke maintains stable pressure to protect surface equipment from pressure fluctuations and prevent premature erosion (high fluids velocities) or abrasion (sand production) on surface equipment or piping components. Additionally, chokes provide the necessary back pressure to a reservoir to avoid formation damage. Other important characteristic, also described by Sachdeva et al. (1986) is regarding the types of single-phase flow regimes developed across the restriction. The first one and most studied is the critical flow, also called choked flow; it occurs when the velocity of the fluids at the smallest area are higher than the sonic velocity. At such conditions, the flow behavior and flow rate across the choke will be dependent only on upstream conditions. Otherwise, the flow is subcritical, and the flowrate depends in both upstream and downstream conditions.

To understand choke valves it is important to study the discharge coefficient (C_d), which is an empirical correlation used as a tool for designing the valves of production systems. This coefficient is used to predict pressure drop and flowrate. The C_d is different for every situation, every choke geometry and opening condition, it is a powerful tuning

instrument. The irreversible losses, heat transfer and model imperfections, are accounted in the discharge coefficient, which in resume depends on the shape of the opening of the restriction (HAUG, 2012).

Furthermore, in flows across restrictions it is common that the minimum area of the jet is often lower than the throat area of the orifice. For this reason, it is necessary to introduce into the mass flow equation a coefficient which will consider the deviations from the theoretical value. (Jobson, 1955 and Omana, 1969). Thus the Coefficient of discharge (C_d) can be defined as a correction term and depends of variables such as: density, viscosity, velocity (those three parameters measured at the orifice), geometry of the inner orifice and choke/pipe diameter ratio. The C_d for the case of a sharp-edge orifice is less than unity, the reasons of that phenomenon is the *vena contracta* which consists in the following: the thick angle at which the boundary layers approach the orifice, makes the fluid continue to converge after leaving it, which forms a smaller cross-section area (*vena contracta*), compared with the orifice inner area. This happens at about one orifice diameter distance downstream of the end of the orifice plate, the boundary layer diverge until the flow returns to be fully developed. This effect is more pronounced at low Reynolds numbers. Figure 1 shows a sketch of the *vena contracta* phenomenon.

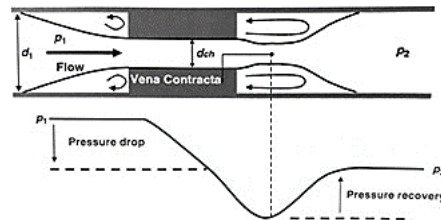


Figure 1. Flow and Pressure behavior of Fluid Flow Across a Restriction (AL-SAFRAN et al. 2017).

Now, it is important to clarify the relationship between choke valves and orifice plates, which explains the reason of the usage of orifice plates as a starting point on the experimental study of this research. The choke valve internal configuration differs among various manufacturers, and even for different valves made by the same company. The internal choke configuration can be fairly complex for the purpose of modeling, because of that, based on Sachdeva's analysis, a choke valve will be treated as a restriction that causes a pressure drop, same as the orifice plate.

Finally, it is important to highlight that Al-Safran et al. (2017) resume the current studies about multiphase flow through restrictions, in two theories: The homogeneous gas-liquid flow models such as: Ashford and Pierce (1975), Sachdeva et al. (1986) and Perkins (1993); and, the theory of nonhomogeneous flow models, such as: Al-Safran and Kelkar (2009), that accounts the slippage between phases. Table 1 presents several works devoted to multiphase flow through choke valves available in the literature.

Table 1. Multiphase Fluid Flow Choke Models.

	Type	Homogeneous / Nonhomogeneous	Fluid Characteristics	Fluid regime	Phase components
Tangren (1949)	Empirical	Homogeneous	isentropic	Critical	
Gilbert (1954)	Empirical			Critical	
Fortunati (1972)	Empirical			Critical / Subcritical	
Ashford and Pierce (1975)	Theoretical	Homogeneous	Isentropic	Critical / Subcritical	
Sachdeva (1986)	Theoretical	Homogeneous	Polytropic	Critical / Subcritical	Air-Water & Air- Kerosene
Perkins (1993)	Theoretical	Homogeneous	Isentropic	Critical / Subcritical	Oil-Water-Natural gas
Schüller (2003)	Theoretical	Nonhomogeneous	Isentropic	Critical / Subcritical	Gas-Water-Oil
Al-Safran and Kelkar (2009)	Theoretical	Nonhomogeneous	Polytropic	Critical / Subcritical	Air-Water mixture

In this work an experimental setup was built to analyze the gas-liquid flow through restrictions such as orifice plates, and then, compare the results with literature models and propose improvements to such models.

2. DESCRIPTION OF THE EXPERIMENTAL SETUP

The test section was built at the Experimental Laboratory of Petroleum (LabPetro) of the Center for Petroleum Studies (CEPETRO) at the University of Campinas (UNICAMP). The entire test section showed in Fig. 2 has a uniform diameter of 19 mm (ID) where the orifice is located at a long enough distance from the inlet to develop the flow. Three orifice plates were designed based on ASME MFC-14M-2008R (Measurement of Fluid Flow Using Small Bore Precision Orifice Meters). The sharp-edged orifice have 1.18 mm thick plate and internal diameters (Bore Size) are 6.4 mm (~16/64 th), 9.53 mm (~24/64 th), and 12.8mm (~32/64 th), all of them chamfered 45° towards the downstream. The setup has been constructed of acrylic pipes to facilitate visual observation and record of the flow phenomena. The working fluids are water and oil (20 cp) and compressed air and are pumped from the storage tank (500 liters) to the inlet section. The liquid flow rate is measured with a Coriolis (Metroval RHM 12). The air is pressurized by a compressor and its flow rate is measured by a Coriolis (MicroMotion CMF15). Both fluids flow through the orifice plate which includes pressure transmitters, differential pressure transmitters and temperature sensors.

The pressure drop in the pipe and across the restriction is measured as shown in **Figure 2**. Based on ASME MFC-14M-2008R three pressure taps are located at different distances: at one diameter upstream the restriction, just at the orifice plate faces (Corner Tappings) and at six diameters downstream the restriction (Recovery Tappings). The error of the instruments are of $\pm 0.5\%$.

During the multiphase flow experiments a high-speed camera is used to analyze the different flow patterns at given liquid and gas mass flow rates and the influence of the singularity on each flow pattern. The multiphase flow patterns are governed by mechanical forces such as: (i) inertia or momentum forces, (ii) gravity force, (iii) viscous force, and (iv) surface tension forces. A carefully analysis of the flow is required to characterize the multiphase flow behavior and to calculate the hydrodynamic parameters like pressure drop and *in situ* velocity. The experimental data can improve the understanding of the phenomena involved and increase the accuracy of models used to predict pressure drop, flow patterns and other multiphase flow characteristics across singularities.

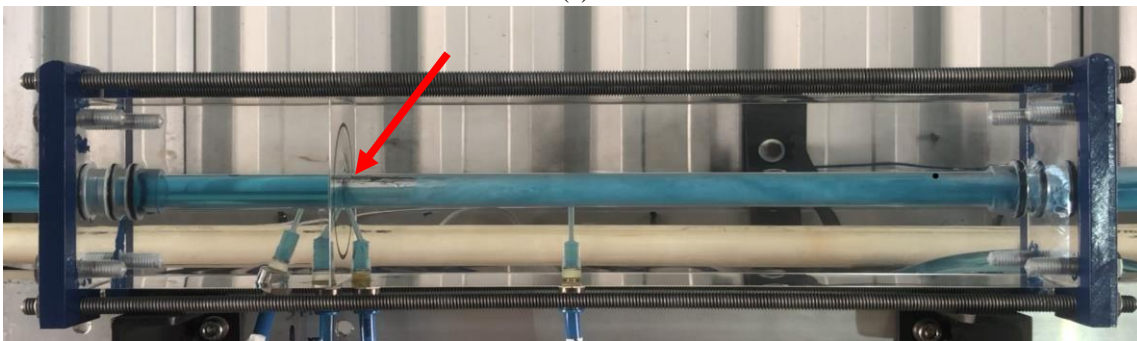
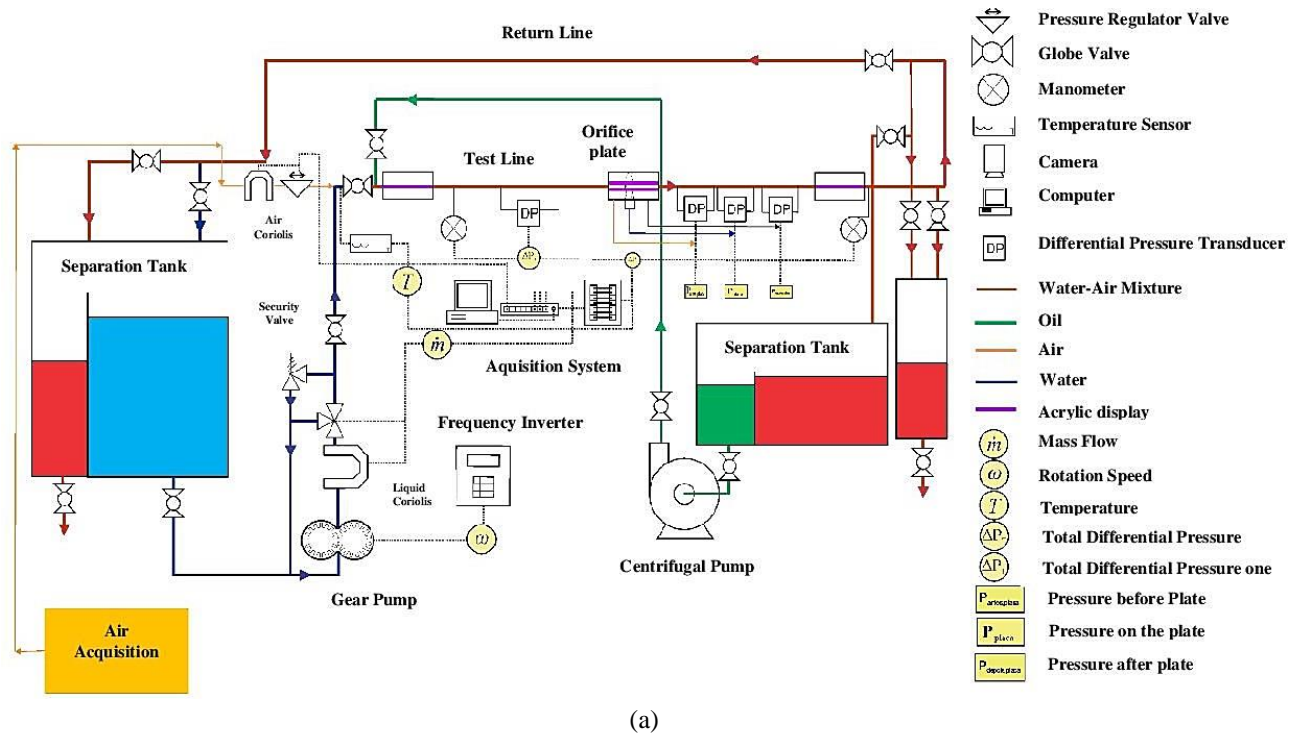


Figure 2. (a) Sketch of the experimental setup at LabPetro/Cepetro – UNICAMP; (b) detail of the visualization box and orifice plate (red arrow).

3. RESULTS AND CONCLUSIONS

The first section shows the results for single-phase water and oil horizontal flows through orifice plates for experimental setup validation purposes. Second the data of two phase flow will be presented (air-water and air-oil). Finally, the flow patterns visualization and an analysis on its influence on the discharge coefficient are performed.

3.1 Single Phase Flow Experiments

The following results are presented based on the Standard ASME regarding single-phase fluid flow through small bore orifice meters (nominal line sizes of $\frac{1}{4}$ inches, through $1\frac{1}{2}$ inches), beta ratio (β) between 0.1 and 0.8 and Reynolds above 1,000. Under this conditions ASME MFC 14M equations are applicable for small bore orifice with corner taps. Equipment calibration and fluid properties had been developed based on ALFA test equipment guidance. Two different fluids were used during this research, these fluids are water and mineral oil (20cP), The figures below cover the results regarding water flow and oil flow tests for orifice plates $16/64^{\text{th}}$ ($\beta= 0.34$), $24/64^{\text{th}}$ ($\beta= 0.5$) and $32/64^{\text{th}}$ ($\beta=0.67$), the mass flow rate range are between 300 to 3.200 kg/h. The limits were obtained base on the experimental setup material (acrylic) and its pressure restrictions.

The results are presented primarily in the form of line plots of predicted mass flow rate [kg/h] vs. measured mass flow rate [kg/h]. In particular, results for the water and mineral oil (20 cP) are shown in Figs. 3 and 4, respectively. Due to the fluid properties, mineral oil was used for flows which run at Reynolds between 150 and 3,500, while water was used to obtain results at higher Reynolds numbers from 5,900 up to 60,000. Table 1 and Table 2 provides a summary of all orifice plates tested for water and for oil flow separately.

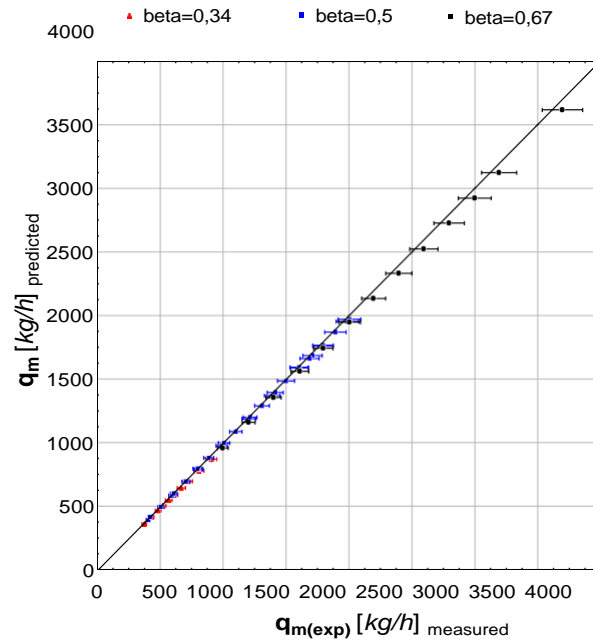


Figure 3. Average horizontal water flow results through orifice plates (ASME MFC 14M)

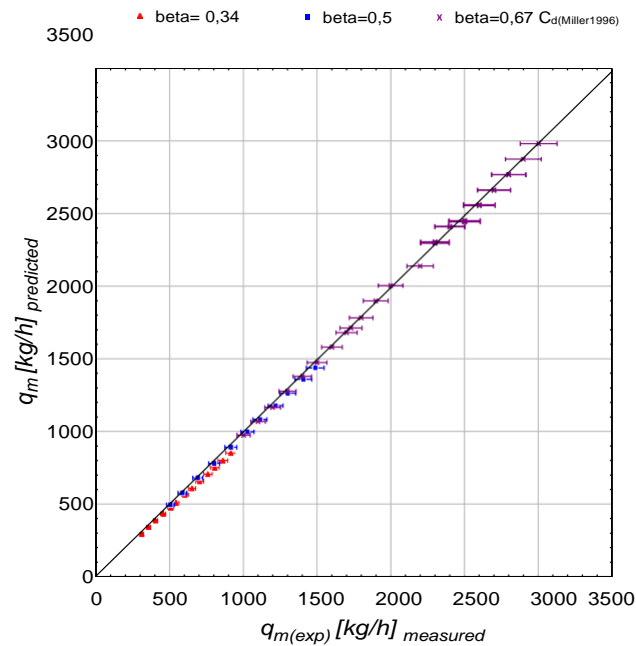


Figure 4 Average horizontal oil flow results through orifice plates

Table 2. Summary horizontal water fluid flow through orifice plate

beta	\dot{m}_{exp} [kg/h]	DP _{exp} [mbar]	\dot{m}_{calc} [kg/h]	error [%]	C _d	Reynolds
0.67±0.01	998±5	43±3	957±43	4	0.63	16000
"	1401±7	87±7	1355±60	3	0.62	22000
"	1796±9	145±12	1742±78	3	0.62	28000
"	2594±13	308±25	2523±113	3	0.62	41000
"	2999±15	415±33	2923±130	3	0.62	48000
"	3695±18	638±51	3618±161	2	0.62	59000
0.5±0.01	404±2	27±2	392±18	3	0.62	6400
"	705±4	86±7	694±32	2	0.62	11000
"	989±5	171±14	976±45	1	0.62	16000
"	1215±6	260±21	1200±55	1	0.62	20000

"	1414±7	351±28	1394±64	1	0.62	23000
"	1892±9	634±51	1869±85	1	0.61	31000
0.34±0.01	374±2	126±10	360±18	4	0.61	5900
"	568±3	288±23	547±28	4	0.61	8900
"	611±3	335±27	590±30	4	0.61	9600
"	721±4	467±37	696±35	3	0.61	11000
"	809±4	583±47	777±39	4	0.61	13000
"	907±5	731±58	870±44	4	0.61	14000

Table 3. Summary horizontal water fluid flow through orifice plate

beta	\dot{m}_{exp} [kg/h]	DP_{exp} [mbar]	T [°C]	\dot{m}_{calc} [kg/h]	Error [%]	C_d	Reynolds
0.67±0.01	3003±15	414±21	30	2980±125	1	0.68 (*)	3500
"	2800±14	357±18	30	2808±116	0.3	0.69(*)	3300
"	2600±13	304±15	30	2629±107	1.1	0.70(*)	3000
"	2400±12	256±13	30	2447±101	2	0.71(*)	2800
"	2199±11	201±10	30	2199±90	0	0.72(*)	2100
"	1500±8	80±4	30	1484±62	1.1	0.77(*)	1600
0.5±0.01	505±3	42±2	20	495±20	2	0.68	380
"	587±3	58±3	20	577±23	2	0.67	440
"	691±3	82±4	20	680±26	2	0.67	520
"	915±5	144±7	20	891±34	3	0.66	680
"	1113±6	215±11	19	1083±41	3	0.66	790
"	1488±7	256±13	19	1438±54	3	0.65	1000
0.34±0.01	309±2	84±4	15	293±12	5	0.66	180
"	401±2	148±7	15	385±16	4	0.65	230
"	503±3	228±11	15	475±19	6	0.65	290
"	600±3	324±16	15	564±23	6	0.64	340
"	699±3	443±22	15	656±27	6	0.64	400
"	911±5	757±38	15	852±34	7	0.64	520

(*) Miller Discharge coefficient $100 \leq Re \leq 10,000$.

It is important to emphasize that one restriction of ASME MFC 14M is that experiments only applies for Reynolds number above 1,000. Most of the tests done with mineral oil run at very low Reynolds number (<103). However, little is known about their discharge coefficient (C_d) values at low Reynolds numbers (Miller, 1996). This is because calibrations for these meters are generally performed in a laboratory using cold water which, at low Reynolds numbers, results in extremely small pressure differentials that are difficult to accurately measure. Consequently, there is a need for accurate low Reynolds number flow measurements for various types of differential flow meters. Therefore, for laminar and transition from laminar to turbulent flow, the discharge coefficient obtained by Miller (1996) was applied. The results of Miller (1996) indicated that the discharge coefficient responded not linearly over the range $100 \leq Re \leq 10,000$.

3.2 Two-Phase Flow Experiments

During this research, two specific theoretical models have been studied for multiphase fluid flow through singularities. The first of them is the non-slip model derived by Sachdeva et al (1986), which is an unidimensional model based on mass, momentum, and energy conservation equations for two-phase gas/liquid mixtures. The second one is the non-homogeneous slip model developed by Al-Safran e Kelkar (2009). Both models are capable of calculating the critical/subcritical flow boundary and the mass-flow rate for critical- and subcritical-flow behaviors. Figures 5 thru 8 presented a comparison between the measured mass flow rate against the predicted flow rate developed through the theory behind these models.

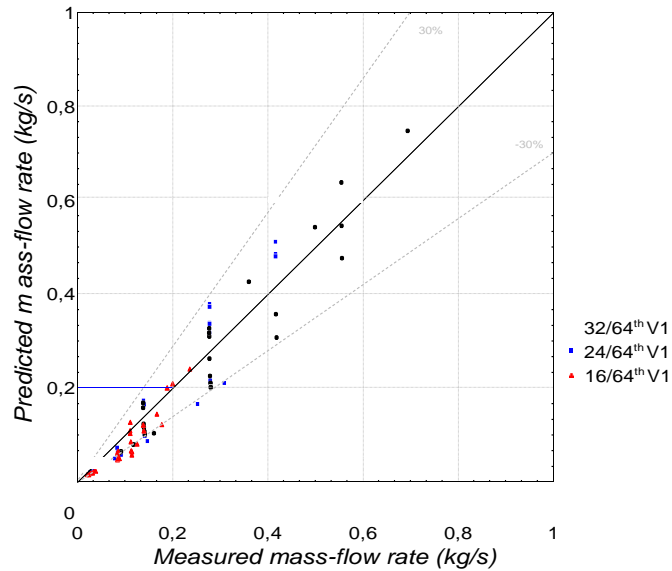


Figure 5 Sachdeva et al (1986) non-slip-model predictions vs. laboratory-measured mass-flow rate (Air – Water Flows).

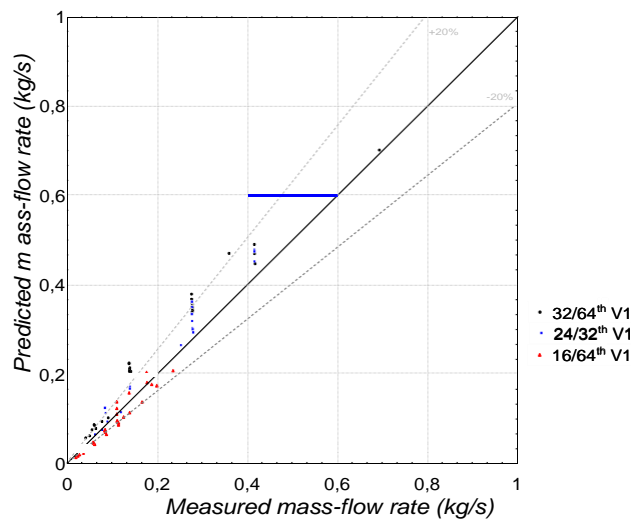


Figure 6 Al-Safran et al (2009) slip-model predictions vs. laboratory-measured mass-flow rate (Air – Water Flows).

It is important to highpoint some of the numerical results and identify some of the experiments with regards to the flow regime and flow pattern, Table 4 resumed some of the experiments about Water-Air flow.

Table 4. Summary Multiphase Fluid Flow Air - Water

beta	Exp. No	'P_1 [kPa]'	'y_c'	Flow Boundary	Flow Pattern	Experimental \dot{m} [kg/s]	Al-Safran (2009) \dot{m} [kg/s]	Sachdeva (1986) \dot{m} [kg/s]
0.34	3	0.06	0.58	Critical	Annular	0.030	0.020	0.0183
"	6	0.04	0.58	Critical	Annular	0.030	0.020	0.0197
"	11	0.11	0.58	Critical	Annular	0.050	0.030	0.0305
"	17	0.05	0.53	Critical	Slug	0.110	0.080	0.0896
"	19	0.03	0.54	Critical	Slug	0.090	0.070	0.0699
"	20	0.04	0.55	Critical	Slug	0.080	0.070	0.059
"	27	0.03	0.42	Critical	Elongated Bubbles	0.110	0.110	0.132

"	28	0.04	0.39	Critical	Elongated Bubbles	0.140	0.130	0.137
"	32	0.08	0.42	Critical	Elongated Bubbles	0.230	0.180	0.225
0.5	41	0.03	0.58	Critical	Annular	0.040	0.040	0.028
"	42	0.03	0.58	Critical	Annular	0.030	0.030	0.022
"	43	0.05	0.55	Critical	Annular	0.140	0.140	0.115
"	46	0.04	0.54	Critical	Slug	0.150	0.140	0.124
"	50	0.03	0.56	Critical	Slug	0.090	0.100	0.0705
"	51	0.03	0.56	Critical	Slug	0.080	0.100	0.0756
"	56	0.04	0.45	Critical	Elongated Bubbles	0.280	0.220	0.281
"	57	0.04	0.46	Critical	Elongated Bubbles	0.270	0.220	0.269
"	65	0.03	0.51	Critical	Elongated Bubbles	0.140	0.150	0.158
0.67	78	0.05	0.58	Subcritical	Annular	0.040	0.040	0.033
"	79	0.04	0.55	Subcritical	Annular	0.140	0.180	0.138
"	80	0.05	0.50	Subcritical	Slug	0.280	0.270	0.294
"	81	0.09	0.50	Subcritical	Slug	0.420	0.360	0.378
"	83	0.08	0.53	Subcritical	Slug	0.280	0.270	0.242
"	92	0.07	0.33	Subcritical	Elongated Bubbles	0.560	0.490	0.673
"	93	0.10	0.33	Subcritical	Elongated Bubbles	0.690	0.560	0.782
"	99	0.06	0.28	Subcritical	Elongated Bubbles	0.550	0.490	0.688

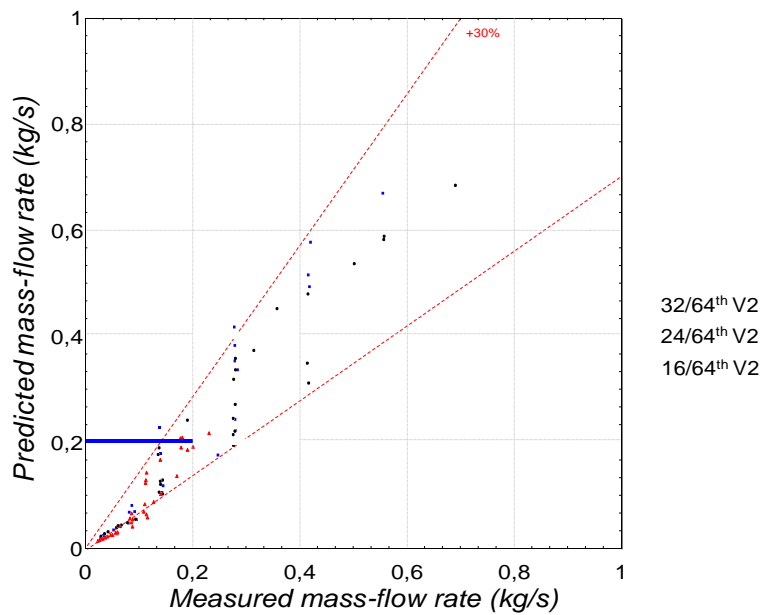


Figure 7 Sachdeva et al (1986) non-slip-model predictions vs. laboratory-measured mass-flow rate (Mineral Oil).

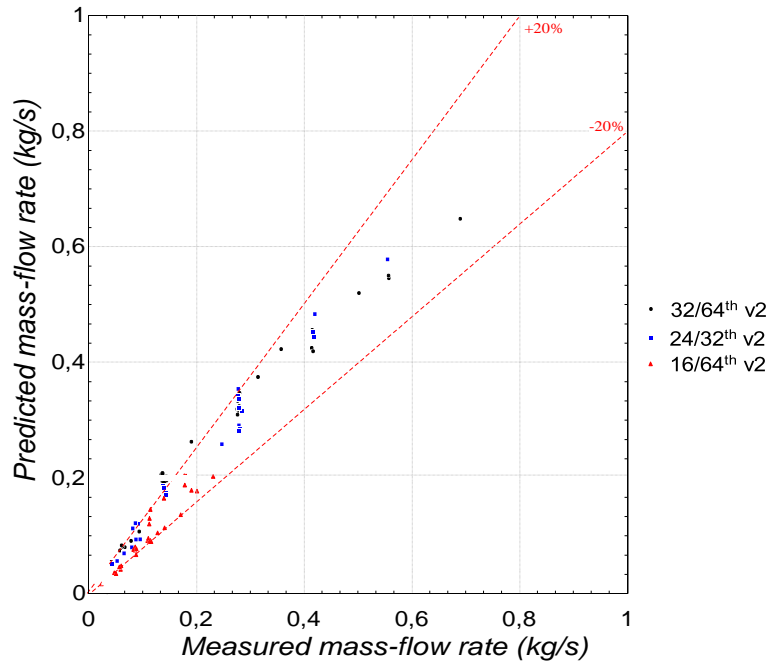


Figure 8 Al-Safran et al (2009) slip-model predictions vs. laboratory-measured mass-flow rate (Mineral Oil).

On based statistical error analysis on Al-Safran et al (2009) this analysis was carried out to calculate the average percent error (E1), absolute average percent error (E2), and standard deviation (E3) for each model. The results of the error analysis are presented in Table 5.

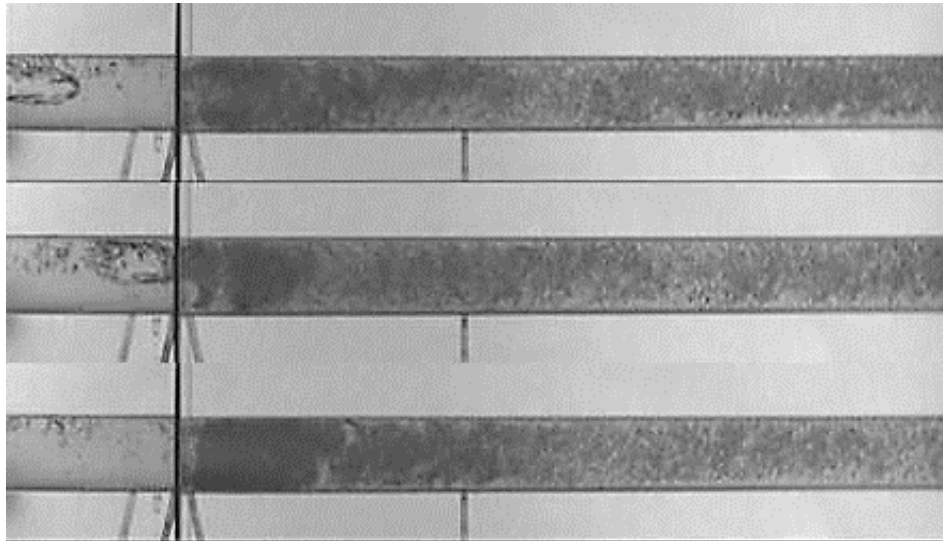
Table 5. Model-Error Analysis

<u>Model</u>	<u>E₁(%)</u>	<u>E₂(%)</u>	<u>E₃(%)</u>
Sachdeva et al (1986) Water-Air	-13%	26%	15%
Sachdeva et al (1986) Oil-Air	-13%	28%	14%
Al-Safran et al (2009) Water-Air	-11%	18%	11%
Al-Safran et al (2009) Oil-Air	8%	18%	12%

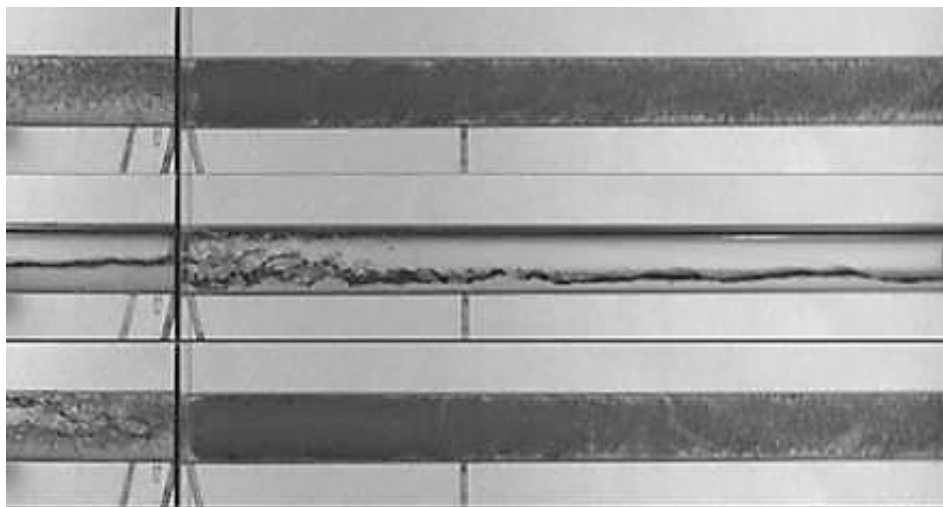
As a resume, in both cases, water-air and oil-air fluid flow, the Elongated Bubbles flow pattern experimental results adjusted better to the theoretical Models, the others two flow patterns not only Annular but also Slug have a different performance. This can be explained due to the amount of air mass flow rate injected on the line and the pressure drop behavior through the orifice plate which is presented in flow visualization and pressure analysis section 3.3.

3.3 Flow Visualization

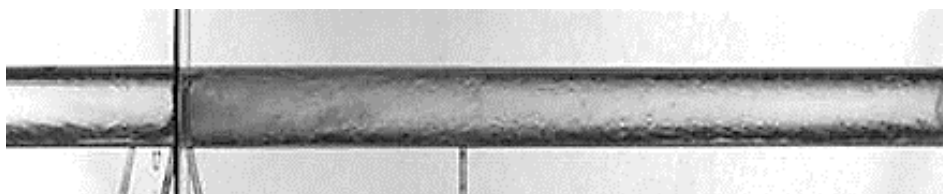
The Figure 9 (a), (b) and (c) presented the three flow patterns obtained during this research. In order to get these images, it was necessary to use a high-speed camera provided by ALFA research group. The camera is triggered so that the video start at the same time as the pressure drop data collection began.



(a)



(b)



(c)

Figure 9 (a) Elongated Bubbles $\beta=0,67$ $0,20\text{m/s}$ Air vs. $0,98\text{m/s}$ Water; (b) Slug $\beta=0,5$ $2,20\text{m/s}$ Air vs. $0,98\text{m/s}$ Water; (c) Annular $\beta=0,3$ 20m/s Air vs. $0,05\text{m/s}$ Water

The video duration was about 5 seconds at 500 FPS, which provides 2,500 pictures for each operational condition. Nearby 200 videos were recorded, half of them for water-oil test the remainder for oil-air test. Almost 70 videos of each flow pattern were collected. The resume of each multiphase flow test is on the Flow Pattern Maps shown in annex 1.

4. CONCLUSIONS

Several conclusions can be summarized based on this study, as follows:

1. The experimental setup was validated for orifice plates flow analysis.
2. The discharge coefficient is highly dependent of fluid properties such as viscosity, density and temperature, especially for low Reynolds (10^2 to 10^4) or high viscous fluids.

3. For low Reynolds numbers the ASME is not able to predict the behavior, as has been stated by the norm. The results obtained by Miller (1996) are similar to the ones we obtained.
4. In the case of single-phase flows, in both water and oil flows the uncertainties between the measured and estimated, through models, mass flow rate are low, inside the uncertainties given by the instrumentation.
5. However, in the case of air-liquid flows, for both air-water and air-oil flows the uncertainties between the measured and calculated mass flow rates are higher than 10% with an spread higher than 20%.
6. The observed flow patterns were elongated bubbles, slug flow and annular flow.
7. Only for the elongated bubbles flow the uncertainties were adjusted by the models.

The results presented here will be used for improvement of models of the literature for pressure gradient and mass flow rate through singularities.

NOMENCLATURE

A : cross sectional area, m²
C_D : discharge coefficient, (nondimensional)
d : choke diameter, m
D : pipe diameter, m
DP: Pressure drop, mbar
γ : gas heat capacity ratio, (nondimensional)
n: polytropic gas expansion coefficient (nondimensional).
P : pressure, Pa
S : slip ratio (nondimensional)
x : mass quality (nondimensional)
 \dot{m} : mass flow rate, kg/s
y: pressure ratio, (nondimensional)
y_c: Critical boundary region
β : diameter ratio, (nondimensional)
ρ : density, kg/m³
c_p: specific heat at constant pressure, J/ (kg K)
c_v: specific heat at constant volume, J/ (kg K)

Subscripts

c : critical
exp : Experimental
g : gas
calc : predicted
o : oil
w : water
1 : upstream
2: at choke throat
3 : downstream

5. ACKNOWLEDGEMENTS

The authors wish to thank PETROBRAS for the financial and technical support in this study. Also, we would like to thank ANP (National Agency of Petroleum, Natural Gas and Biofuels) for the support through its "Compromisso de Investimentos com Pesquisa e Desenvolvimento". We would also like to thank the School of Mechanical Engineering (FEM) and the Center for Petroleum Studies (CEPETRO) both at the University of Campinas (UNICAMP). Acknowledgements are extended to CAPES – Brazilian Federal Agency for Support and Evaluation of Graduate Education within the Ministry of Education of Brazil for Mr. Luiz Ojeda's scholarship. We would finally like to thank the ALFA research group for their support.

6. REFERENCES

AL-SAFRAN, E.M. e BRILL, J.P., Applied Multiphase Flow in Pipes and Flow Assurance. SPE Textbook Series, 2017. Chap. 2, p.123-139.

- AL-SAFRAN, E.M. e KELKAR, M., Predictions of two-phase critical-flow boundary and mass-flow rate across chokes. *SPE Production & Operations*, 2009. Vol. 24, No. 2, pp. 249–256.
- ANDREOLLI, Ivanildo. “Introdução à elevação e escoamento monofásico e multifásico de petróleo”. Editora Interciência, Rio de Janeiro, Chap 5, p. 311-397. 2016.
- ASHFORD, F. E. et al. Determining multiphase pressure drops and flow capacities in down-hole safety valves. *Journal of Petroleum Technology*, v. 27, n. 09, p. 1,145-1,152, 1975.
- BRILL, James P.; BEGGS, Howard Dale. *Two-phase flow in pipes*. 1991.
- GILBERT, W. E. et al. Flowing and gas-lift well performance. In: *Drilling and production practice*. American Petroleum Institute, 1954.
- HAUG, Ragnhild Krogsrud. *Multiphase Flow Through Chokes-Evaluation of five models for prediction of mass flow rates*. 2012. Dissertação de Mestrado. NTNU.
- MAIDANA, Nathan da Costa, *Perturbações induzidas por uma placa de orifício no escoamento horizontal de ar e água no padrão intermitente*, Dissertação de Mestrado, Campinas, SP, 2017.
- MANDHANE, G.A. Gregory, K. Aziz, A flow pattern map for gas—liquid flow in horizontal pipes, *International Journal of Multiphase Flow*, Volume 1, Issue 4, 1974,
- MILLER, R.W., *Flow Measurement Engineering Handbook*, Third ed. McGraw-Hill Companies, Inc., Boston, MA. 1996.
- PERKINS, Thomas K. et al. Critical and subcritical flow of multiphase mixtures through chokes. *SPE Drilling & Completion*, v. 8, n. 04, p. 271-276, 1993.
- ROS, N. C. J. An analysis of critical simultaneous gas/liquid flow through a restriction and its application to flowmetering. *Applied Scientific Research*, v. 9, n. 1, p. 374, 1960.
- SACHDEVA, R. et al. Two-phase flow through chokes. In: *SPE Annual Technical Conference and Exhibition*. Society of Petroleum Engineers, 1986.
- SCHÜLLER, R. B. et al. Evaluation of multiphase flow rate models for chokes under subcritical oil/gas/water flow conditions. *SPE production & facilities*, v. 18, n. 03, p. 170-181, 2003.
- TANGREN, R. F.; DODGE, C. H.; SEIFERT, H. S. Compressibility effects in two-phase flow. *Journal of Applied Physics*, v. 20, n. 7, p. 637-645, 1949.

7. RESPONSIBILITY NOTICE

The authors are the only responsible for the printed material included in this paper.

8. APPENDIX A

The data base collected for study the multiphase models is present on the following flow pattern maps. The map used on this study was developed by Mandhane (1974).

Figure A-1 is the oil-air flow pattern map, and Figure A-2 is the water-air flow pattern map. The symbols inside each flow map represents the experimental points of each orifice plate.

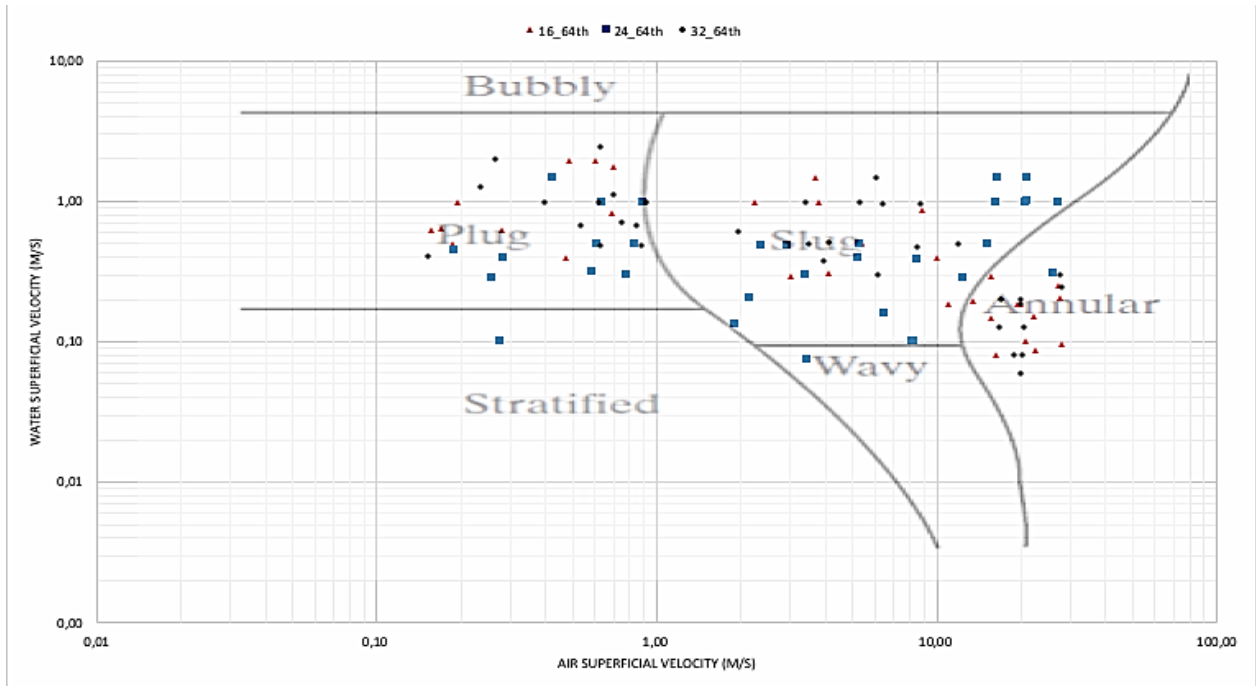


Figure A-1 Flow Pattern Map for Oil – Air Flows (Madhane, 1974)

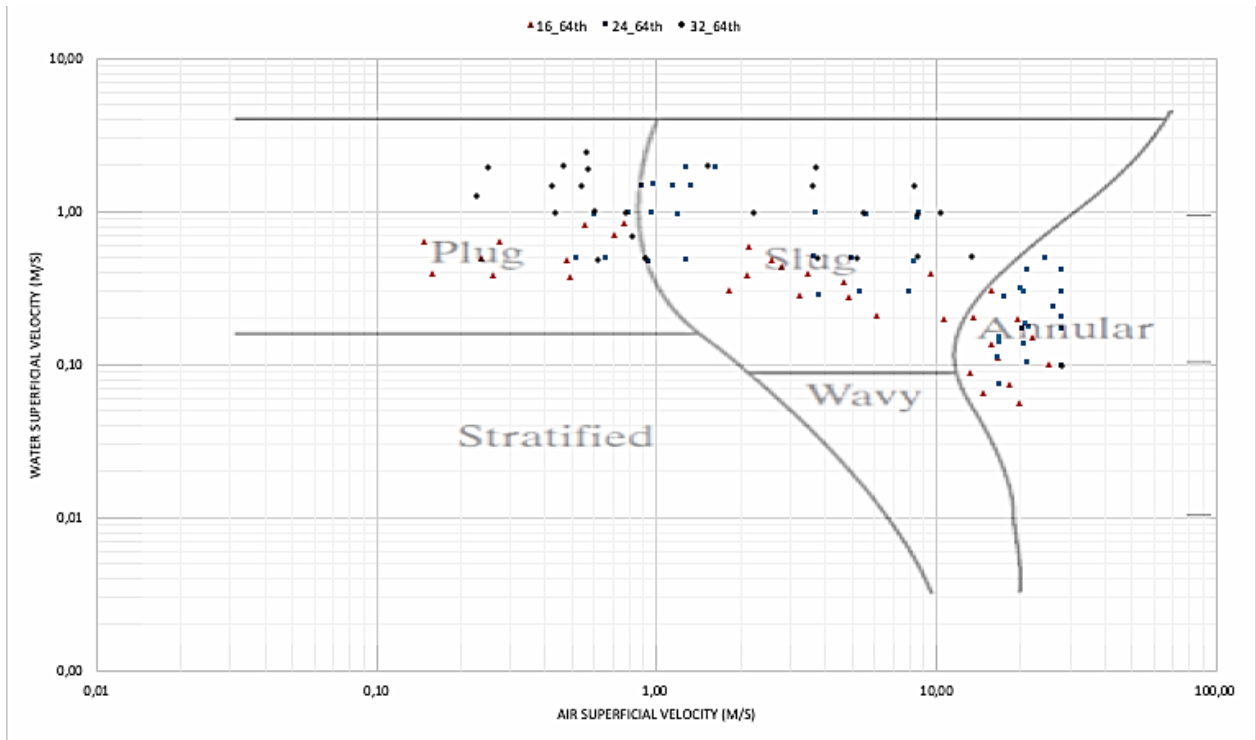


Figure A-2 Flow Pattern Map for Water – Air Flows (Madhane, 1974)